ELSEVIER

Protocol

In vivo preparation and identification of mitral cells in the main olfactory bulb of the mouse

Thomas G. Mast*, Edwin R. Griff*

Department of Biological Sciences, University of Cincinnati, Cincinnati, OH 45221-0006, USA

Abstract

The mouse main olfactory bulb (MOB) is commonly used as a mammalian model to study olfactory processing. The genetic techniques available with the mouse make its MOB a powerful model for analysis of neuronal circuitry. The mouse has been used as a mammalian model for all types of MOB neurons, but especially to study the activity of mitral cells. However, mouse mitral cell activity is most commonly studied in vitro. Therefore, we aimed to develop a protocol to record the activity of antidromically identified mitral cells in mouse in vivo. Currently, such a protocol does not exist. Using extracellular techniques, we report a protocol that is able to record neurons from all mouse MOB layers. Specifically, mitral cell single-units were identified by antidromic activation from the posterior piriform cortex, and their spontaneous activity was recorded for more than 30 min. This protocol is stable enough to record from single-units while buprenorphine was applied both topically to the surface of the MOB and injected systemically.
© 2005 Elsevier B.V. All rights reserved.

1. Type of research

The mammalian frontal cortex receives information about the chemical environment through connections from the main olfactory bulb (MOB). The electrophysiology of the principal output neurons of the MOB, mitral cells, has primarily been studied in vivo in rat [4,26,34,36,43,44] and rabbit [11,18,30]. Detailed analysis of MOB circuitry and pharmacological manipulations of mitral cell membrane physiology have primarily occurred in mouse and neonatal rat in vitro models [1,9,21,26]. In vitro brain slice preparations are able to maintain relatively stable physiology, including spontaneous activity [5,27]; however, this activity

may be altered by a loss of input from several classes of neurons. In rat, in vitro recordings of mitral cell spontaneous activity average about 3 Hz [5], while in vivo recordings average about 30 Hz [16]. The mouse is an attractive model for physiology because of the many specific genetic alterations available [3,4,23,32]. An in vivo mouse model would facilitate analysis of MOB circuitry and mitral cell membrane physiology in an intact and genetically alterable system.

Mitral cells can be identified in vivo by antidromic activation from the posterior piriform cortex (pPC), since only mitral cells project from the MOB to this region [12,34,36,37]. However, the invasive surgery and the small size of the mouse have presumably deterred the development of a protocol for recording from mitral cells in vivo in mouse. Although mouse in vivo techniques are becoming more common [3,7,8,17,21,22,32], a protocol to record antidromically identified mitral cells in mouse does not exist. This protocol describes the anesthetic and surgical

* Corresponding authors. Thomas G. Mast is to be contacted at fax: +1 513 558 1885. Edwin R. Griff, fax: +1 513 556 5299.
  E-mail addresses: masttg@hotmail.com (T.G. Mast), edwin.griff@uc.edu (E.R. Griff).

procedures necessary for studying mouse mitral cell physiology in vivo. We tested the usefulness of the protocol by characterizing 6 mitral cells and by observing the effect of the pharmacological agent buprenorphine.

2. Time required

Depending on the specific goal, and including the inherent variability of in vivo experiments, each experiment will last 4–12 h.

2.1. Surgical preparation: 30–65 min from induction of anesthesia to ground electrode insertion

(a) Induction of anesthesia, shave surgery site, subcutaneous injections of lidocaine: ~10 min. In some animals, induction is problematic and requires additional injections of anesthesia: extra 10–30 min.
(b) Insertion of intraperitoneal tube, insertion of rectal thermometer, and incision of scalp: <10 min.
(c) Insertion of ground electrode: <10 min.

2.2. Surgery: 75–150 min

(a) Placement of animal in stereotaxic: <5 min.
(b) Insertion of EEG electrode: 15–25 min.
(c) Exposure of dorsal MOB: 15–40 min.
(d) Exposure of posterior piriform cortex: 40–90 min.

2.3. Recording set-up: 15 min

(a) Electrode set-up: 12 min.
(b) Clean airline: <3 min.

2.4. Recording: most variable, dependent on experimental design: 2–10 hrs

(a) Location and recording of single-units based on extracellular techniques: minutes to hours (based on experimental design).

3. Materials

3.1. Animals

All procedures in this study are in accordance with federal animal care guidelines and were approved by the University of Cincinnati Institutional Animal Care and Use Committee. Animals were housed in filtered, clear plastic cages on a 12-h light/dark cycle. Food and water were provided ad libitum. Generally, mice were ICR females or C57BL6J (B6) males weighing between 19 and 40 g (Harlan; Indianapolis, IN). However, both sexes in both strains have been used successfully with this protocol.

3.2. Special equipment

(a) Micropipette puller: Sutter Instrument Co. (Model p-80; San Francisco, CA).
(b) Stereotaxic frame and microelectrode micropositioner: David Kopf Instruments (Model 1640, Model 650; Tujunga, CA).
(c) Pre-amplifier and window discriminator: Dagan (Model 2400a and Model WD-2; Minneapolis, MN).
(d) Oscilloscopes and amplifiers: Tektronix (Model 5111A, Model 5A22N; Gaithersburg, MD).
(e) Stimulation and isolation units: Grass (Model S44, Model SIU5; West Warwick, RI).
(f) Data acquisition hardware and software: Cambridge Electronic Design (Model µ1401, Spike2 ver4.0; Cambridge, UK).
(g) Analog-to-digital data storage: Medical Systems (Model PCM-8; Greenvale, NY).
(h) Stimulation and EEG electrode wire: California Fine Wire (0.125 mm stainless steel insulated wire; Grover Beach, CA).
(i) Micropipette glass: World Precision Instruments (Item 1B15OF-4; Sarasota, FL); pulled to 5–10 MΩ resistance.
(j) Teflon and glass tubing for delivery of clean air.
(k) Dental drill: Fordom electronic company (Model 73; Bethel, CT).
(l) Dental burs: SS White (Model HP-35; Lakewood, NJ).
(m) Polyethylene tubing: Becton Dickinson (Intramedic PE10: I.D. 0.28 mm, O.D. 0.61 mm; Sparks, MD).
(n) Water heater and pump: Gaymar Industries, (Model TP-500; Orchard Park, NY).

3.3. Chemicals

(a) Chloral hydrate and lidocaine: Sigma (St. Louis, MO).
(b) Buprenorphine: Reckitt Benckiser (Buprenex; Richmond, VA).
(c) Dental acrylic: Lang Dental (Jet; Wheeling, IL).

4. Detailed procedure

4.1. Anesthesia

Anesthesia was induced by an i.p. injection of 4% chloral hydrate solution at a dose of 400 mg/kg. Additional doses of anesthesia at 40 mg/kg were administered via a polyethylene (PE) tube inserted into the abdominal cavity. The tubing was inserted using an 18-gauge needle to pierce the abdominal wall; the tubing was fitted inside the needle. After the needle was retracted, the tubing was sutured to the skin. The tube was connected, via a blunted 30-gauge needle inserted into the PE tubing, to a syringe filled with chloral hydrate.

Chloral hydrate was chosen to provide long-term (up to 12 h), relatively stable anesthesia; gastrointestinal and/or liver complications are not relevant since this is non-recovery surgery. The EEG (see below), respiration rate, and response to a toe pinch (withdrawal reflex) were recorded about every 30 min to monitor the plane of anesthesia. The plane of anesthesia was maintained such that a pinch did not elicit a withdrawal reflex, but did desynchronize the EEG.

Under anesthesia, the respiration rate varied from 60 to over 200 breaths/min. The lower value was common during deep anesthesia required for surgery; higher values were maintained during recording, typically around 150 breaths/min. This value is similar to the normal, awake resting respiratory rate of approximately 163 breaths/min in the laboratory mouse [15].

4.2. Surgery

The following steps were undertaken in preparation for surgery after anesthesia induction. The head was shaved of fur and lidocaine was administered s.c. to the dorsal scalp, neck, and facial muscles. Local anesthesia, administered prior to incisions, minimizes the risk of pain in the extensive surgery necessary to expose the piriform cortex. A rectal thermometer probe (YSI; Yellow Springs, Ohio) was inserted and secured to the tail with tape. The dorsal skull was exposed with a midline incision from snout to neck. A silver ground electrode was inserted into the neck muscles and affixed with suture. The mouse was then placed in a stereotaxic adapted for a mouse with a snout holder and a Plexiglas trough to hold the animal. Body temperature was maintained with a circulating-heater. A Plexiglas water-bath was built to fit under the trough and was connected to a water heater and pump; it kept the animal at 34.5 to 35.5 °C.

An EEG electrode was implanted in the parietal cortex. A 1- to 2-mm-diameter area of parietal bone was thinned with a dental bur, and the bone and dura were removed with fine forceps. A small steel post (a small, inverted nail) was affixed to the bone with super-glue about 1 mm from the opening. A bipolar electrode made from 75-μm stainless steel wire, cut at a 45° angle to offset the tips, was positioned in the cortex. The more superficial of the two tips was positioned about 100 μm below the cortical surface. The exposed cortex was covered with artificial cerebral spinal fluid (ACSF)-dampened cotton. The electrode was affixed to the steel post and the parietal bone with dental acrylic.

The dorsal surface of the MOB was exposed (Fig. 1A). A window in the frontal bone was thinned with a dental drill and bur (diameter = 1.0 mm). The 4–6 mm^2 opening was limited medially by the sagittal suture, rostrally by the stereotaxic snout-holder, laterally by the orbit, and caudally by the rostral dorsal cerebral vein. The bone and dura were removed with fine forceps. During subsequent surgery and recording, the exposed MOB was kept moist with ACSF-dampened cotton.
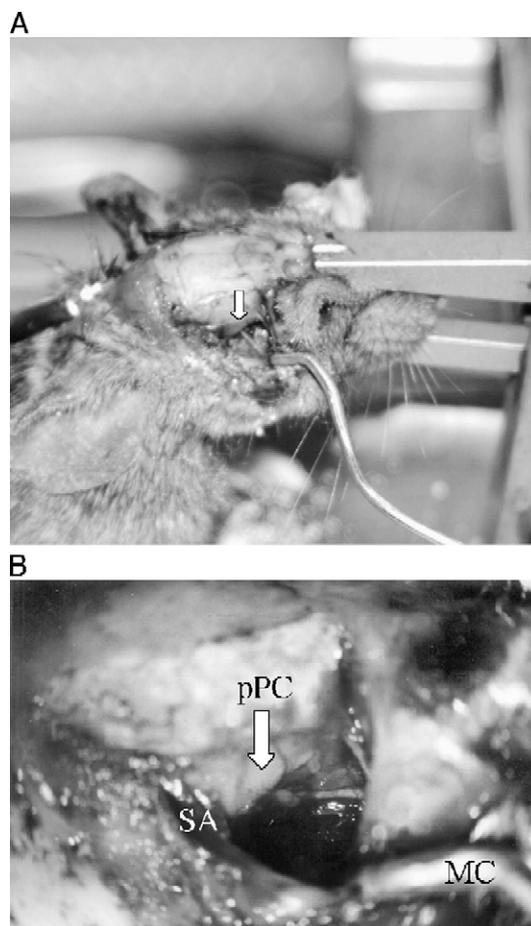

Fig. 1. The surgery. In panel A, the animal is in the stereotaxic and is ready for recording. A window to the pPC has been exposed after removing the muscles (arrow), skin, and TMJ of the lateral skull. Panel B is a close-up of the dissection. Note the metal clip depressing the jaw (MC), and the large stapedial artery (SA) caudal to the TMJ at the far left of the image. The posterior portion of the lateral olfactory tract is seen as a white triangle in the exposed posterior piriform cortex (pPC; arrow). The middle cerebral artery is also visible.

To expose the pPC, an incision exposed the facial muscles extending from the parietal bone, caudal to the eye, to the jaw. The muscles were then stripped away to expose the zygomatic arch. The arch was removed with fine diagonal cutters. The temporal mandibular joint (TMJ) was exposed and the joint capsule was removed with forceps. The stapedial artery is attached to the medial–caudal surface of the TMJ capsule; care must be taken not to tear this artery (Fig. 1B).

Next, the jaw was depressed and held in this position for the entire recording period using a steel hook and an elastic band. The basisphenoid bone inferior to the zygomatic process and caudal to the middle cerebral artery was thinned. The bone and dura were removed with fine forceps. The exposed piriform cortex and lateral olfactory tract (LOT) were kept moist with a small pool of ACSF. Care was taken to open as large a window as the vasculature would allow (Fig. 1B). Note: this portion of the surgery can

be omitted if antidromic stimulation of mitral cells is not required.

4.3. Recording set-up

To obtain stable recordings, the animal in the stereotaxic was placed within a grounded Faraday cage; one recording and two stimulation electrodes were positioned. One stimulation electrode was for orthodromic activation of the MOB. This was a bipolar electrode made of 0.125 mm stainless-steel wire (California Fine Wires; Grover Beach, CA), insulated except for the cut tip. The tip was cut flat using a single-edged razor blade and polished with a whetstone. The electrode was positioned such that the tip contacted the olfactory nerve layer (ON) at the far rostral end of the MOB.

The second stimulation electrode was for antidromic activation of the MOB from the piriform cortex. This was a bipolar electrode made of 0.125-mm stainless-steel wire in which 500–700 μm at the end was bent 90° and the outer face flattened with a whetstone, also removing the insulation. This face was placed against the posterior piriform cortex. To facilitate electrode placement, the stereotaxic apparatus was tilted about 30° throughout the recording session.

The recording electrodes were made from borosilicate glass pipettes ('Dot glass' 1.0 mm O.D., 0.7 mm I.D., WPI; Sarasota, FL); electrodes were pulled to a tip diameter of 1–3.0 μm, filled with 2% pontamine blue/0.5 M sodium acetate, and had a final resistance of 5–10 MΩ. An area of the exposed bulb was selected where stimulation from orthodromic and antidromic electrodes evoked field potentials. To record field potentials, the recording electrode was positioned about 50 μm below the surface of the MOB using a hydraulic micropositioner (David Kopf Instruments; Tujunga, CA). Field potentials were typically evoked by square wave pulses of current 10–100 μs in duration, 70–400 μA. Stimulation pulses were generated by a stimulator and isolated from ground (S44, SIU5, Grass Instruments; West Warwick, RI).

4.4. Experimental procedure

4.4.1. Single-unit isolation

In these preliminary experiments, MOB single-unit spontaneous activity was recorded, including mitral cells. To ensure that the activity was spontaneous (i.e., activity in the absence of odor stimulation), laboratory odors were blocked with clean air. Medical-grade air was further purified by passing it through activated charcoal, a molecular sieve, and then humidified by bubbling through distilled water. The purified air was directed at the nares at a flow rate of about 400 ml/min. Before reaching the nares, purified air came in contact with only glass, water, and Teflon.

MOB single-units were found, identified, and isolated using extracellular recording techniques. When locating single-units online, first the desired MOB cellular layer was identified by its depth and position relative to the mitral cell layer. The mitral cell layer was the depth at which the prominent negative-going component of the field potential, evoked by either orthodromic or antidromic activation, reversed polarity [4,13,34,36,43]. The remaining layers were identified as being either superficial (glomerular, external plexiform) or deep (internal plexiform, granule) to the mitral cell layer. Depth was measured in micrometers from the MOB dorsal surface using the travel distance on the micropositioner. Units were then found by observing spontaneous action potentials (amplified 1000×) on an oscilloscope, listening for spontaneous action potentials through a speaker, and/or by observing action potentials evoked by antidromic stimulation from the posterior piriform cortex. Antidromic activation is the only way to locate mitral cells that lack spontaneous activity; it is also helpful in identifying neurons with slow or irregular patterns of action potentials. Action potentials were considered to originate from a single neuron (single-unit) if they maintained constant shape, constant amplitude, and an interspike interval of at least 2 ms [43]. Isolated units from the mitral cell layer were then tested for antidromic activation from the posterior piriform cortex. Square wave pulses (200–300 μs; 70–400 μA) from the posterior piriform cortex were used to evoke an action potential from the isolated unit, and the latency of this antidromically-evoked action potential was recorded. Lastly, to confirm that a unit projects to the pPC, a collision test was performed.

A collision test demonstrates that a spontaneous action potential is being generated by the same neuron whose axon is excited antidromically; in this case, an axon that projects to the posterior piriform cortex [34,36,44]. In a collision test, spontaneous action potentials are used to trigger the antidromic stimulation after a preset delay. If the stimulus is delivered after a delay longer than the conduction time for an action potential between the recording and stimulating sites, the antidromic action potential is observed. When the stimulus is set for a shorter delay, the antidromic action potential collides with the spontaneously driven action potential, and is blocked. After the activity of a unit was recorded, pontamine blue dye was electrophoretically ejected from the tip of the recording electrode to mark the actual recording site (−10 μA current, 7 s on/3 s off duty cycle for 10 min).

4.4.2. Single-unit recording

After isolating a single-unit, the spontaneous activity was recorded. Action potentials were filtered between 300 and 3000 Hz, and stored digitally on magnetic tape (Medical Systems; Greenvale, NY). The signal was also passed through a window discriminator (Dagan; Minneapolis, MN), and each discriminated action potential stored as an event on a PC (μ1401, Spike2 software, CED; Cambridge, UK).

Mitral cell single-units were characterized as follows. Mitral cell spontaneous activity was recorded for several

minutes to establish a stable and artifact-free baseline. Spontaneous activity and latency were chosen to preliminarily characterize these cells. Spontaneous activity was calculated as the mean firing rate of 200 s of continuous firing. Latency was calculated as the mean time required for an antidromically driven action potential to travel from the piriform cortex to the cell body. The time was measured from the stimulus artifact to the peak of the action potential. This was repeated for several cycles and the times were averaged. The rounds of stimulation required to measure the latency of a unit were concluded several minutes before the recordings spontaneous (non-stimulated) activity began.

4.4.3. EEG recording

To measure the plane of anesthesia, the EEG was recorded. The EEG signal was filtered DC to 30 Hz. The signal was then passed to a chart recorder for visualization. The EEG was also stored on magnetic tape (Medical Systems) and on a PC digitized at 100 Hz (μ1401, Spike2 software, CED; Cambridge, UK).

4.4.4. Buprenorphine

The partial μ-opioid receptor agonist buprenorphine (Buprenex, Reckitt Benckiser; Richmond, VA) was used to test the model for the application of pharmacological agents. Buprenorphine is commonly used as an analgesic in laboratory animals [33] and was chosen for two reasons. First, chloral hydrate may [10] or may not [39] provide adequate analgesia during surgery. Consequently, our lab and university veterinarians are interested in analgesic supplements to chloral hydrate anesthesia. Second, pharmacological agents are useful tools in studying the MOB. They can be used to investigate the role of receptors and their ligands in MOB circuitry. Although the pharmacology of buprenorphine is complex, including interactions with μ-, δ-, κ-opioid, and opioid-like receptors [6,19], at low doses buprenorphine is an μ-opioid receptor agonist [6,19]. μ-Opioid receptors are expressed in the MOB [35,40] and buprenorphine can inhibit MOB single-unit activity (unpublished data). For these reasons, buprenorphine was chosen to test this protocol for the application of pharmacological agents.

Buprenorphine was injected s.c. to test a systemic route of administration for pharmacological agents. Some pharmacological agents, such as the glutamate agonist kynurenic acid, are effective when applied topically [29]. However, topical application of pharmacological agents can be disruptive during single-unit recording. Buprenorphine was also applied topically with a digital pipette in 10- to 50-μl aliquots during single-unit recordings. These tests were conducted to demonstrate the recording stability of the model. For controls, dextrose (50 mg/ml) was applied both s.c. and, along with ACSF, directly to the MOB surface. ACSF was prepared as previously described [1].

5. Results

5.1. Spontaneous activity

Histologically, the mammalian MOB has five distinct layers with different neurons found in each. Using the above protocol, single-unit spontaneous activity in each layer was identified and recorded in both ICR and B6 mice as shown in Table 1. The top tier of Table 1 lists the recorded single-units by both MOB layer and strain of mouse. The emphasis of this protocol was to record the spontaneous activity of single-units from the mitral cell layer. To confirm online that units recorded from the mitral cell layer were indeed mitral cells, electrical stimulation of the pPC was used to drive single-units and collision tests were performed (Fig. 2). Mitral cell single-unit spontaneous activity was routinely maintained for over 30 min (Fig. 3). Mitral cell single-units from both ICR and B6 mice were identified and characterized. The bottom tier of Table 1 lists 6 such units by strain. The protocol was used on the hardier outbred ICR and the isogenic B6. The inbred strain B6 is a common genetic background for transgenic and gene-knockout techniques.

5.2. Effect of buprenorphine

Buprenorphine was used to test if the protocol could detect changes in MOB activity induced by pharmacological agents and if those agents could be administered systemically and topically. Both systemically (Fig. 4A) and topically applied (Fig. 5A) buprenorphine decreased the spontaneous activity of single-units found near the mitral cell layer. Buprenorphine vehicle did not have an effect (Figs. 4B and 5B, respectively). For the length of each

Table 1
Histologically-confirmed cells

Layer	ICR	B6
Glomerular	2	0
Epl	5	2
Ipl	7	0
Granule	1	0
Mitral	8	8

Antidromically-driven mitral cells

Strain	Rate (Hz)	Latency (ms)
ICR	36.6	3.01
ICR	13.5	1.81
B6	14.23	2.99
B6	8.91	2.65
B6	17.48	3.69
B6	9.68	2.56

The top tier lists the number of cells recorded in each mouse strain based on dye-spot location. Note that mitral cells could be recorded in each strain. The bottom tier lists 6 confirmed mitral cells by strain, mean rate of spontaneous activity, and latency between stimulation of pPC and the peak of the antidromic action potential in the MOB. Abbreviations: Hz: hertz; ms: milliseconds.
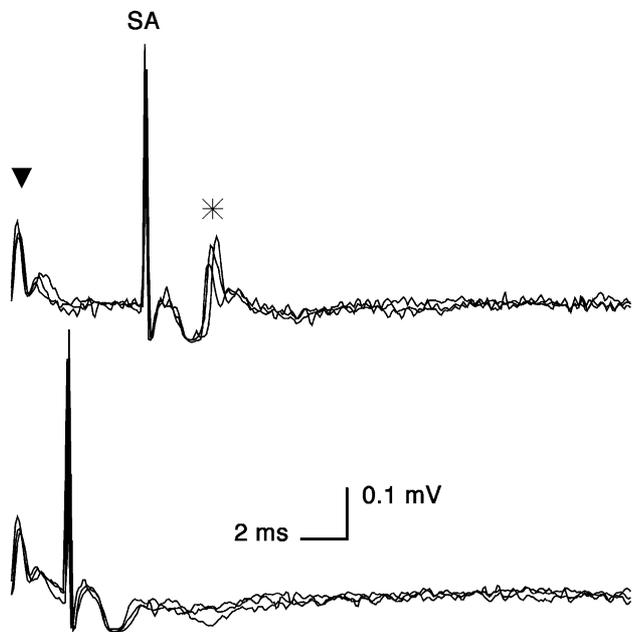
Fig. 2. Collision test. The top trace shows 3 superimposed responses evoked by square-wave stimulation (SA, the resulting stimulus artifact) from the pPC triggered by spontaneous spikes (down arrowhead) with a 5-ms delay between the spontaneously generated action potential and stimulation. The result is an antidromic spike (asterisk). In the bottom trace, the delay is decreased to 2 ms. Note the antidromic spike is absent because it collided with the spontaneously generated action potential.

recording, the unit activity was clearly isolated and was not drifting away. Topically applied ACSF did not affect single-unit spontaneous activity (data not shown).

5.3. Effect of chloral hydrate

While developing the protocol, the inbred and outbred mice were observed to be differentially sensitive to chloral hydrate. Compared with ICR mice, the B6 mice were more prone to accidental overdose (7 and 27%, $N=72$ and 41, respectively). Furthermore, some B6 mice had little sponta-
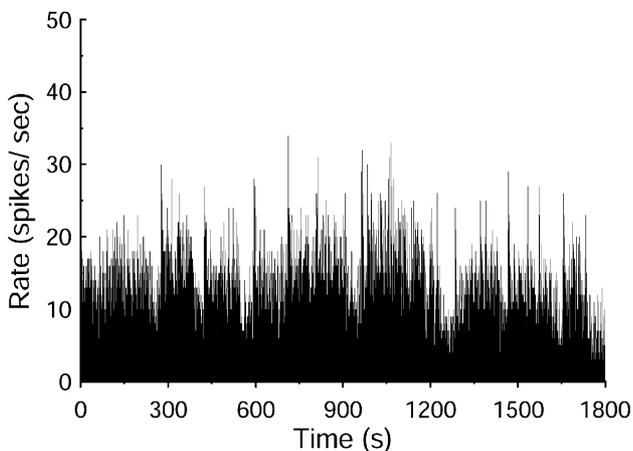

Fig. 3. Single-unit spontaneous activity. A ratemeter histogram displaying 30 min of spontaneous activity from an antidromically-identified single-unit from an ICR mouse.
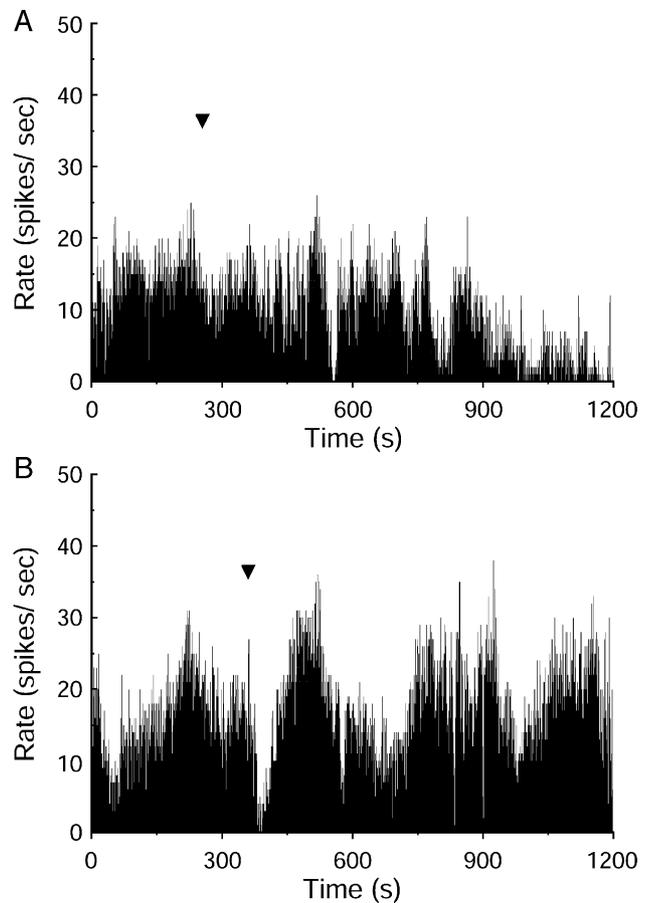

Fig. 4. Effect of systemic buprenorphine. In panel A, buprenorphine at 0.02 mg/kg was injected s.c. (down arrowhead) during a MOB single-unit recording in an ICR mouse. The spontaneous activity of this unit decreased over the following 900 s. The unit recording was lost before the unit could recover. In panel B, 50 mg/ml glucose (vehicle) was injected s.c. (down arrowhead) during a MOB single-unit recording in an ICR mouse. The robust and oscillating spontaneous activity continued to be unaffected for the next 900 s.

neous single-unit activity, yet normal stimulus-evoked field potentials (data not shown). The field potential is the sum of the excitatory and inhibitory postsynaptic potentials, and the large negative-going component primarily reflects the excitatory synapses [1,29]. A reproducible field potential indicates working synapses [1].

6. Discussion

6.1. Assessment of the protocol

This protocol provides a method for recording from the mouse MOB in vivo using extracellular techniques. Under experimental conditions, all layers of the MOB were spontaneously active. Most importantly, in the anesthetized mouse, the pPC can be surgically exposed. This exposure allows mitral cells to be identified by antidromic activation. Lastly, the effects of pharmacological agents can be measured after both systemic and topical administrations.
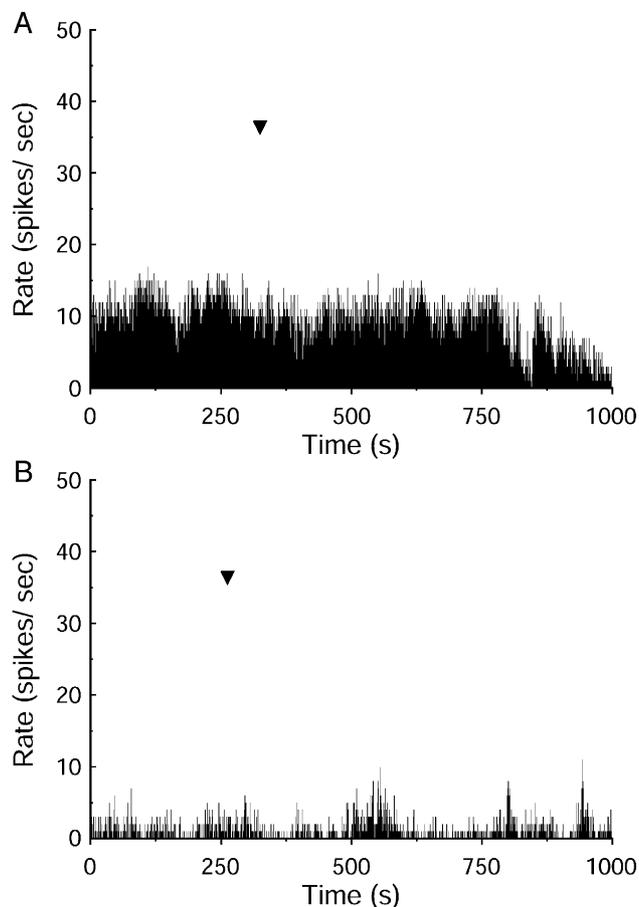
Fig. 5. Effect of local buprenorphine. In panel A, buprenorphine at 0.02 mg/kg was applied directly to the MOB surface (down arrowhead) while recording a MOB single-unit in an ICR mouse. The spontaneous activity of this unit decreased over the following 600 s. The unit recording was lost before the unit could recover. In panel B, 50 mg/ml glucose (vehicle) was applied directly to the MOB surface (down arrowhead) while recording a MOB single-unit in an ICR mouse. The spontaneous activity of unit continues to be unaffected for the next 600 s. Both buprenorphine and vehicle were applied at a volume of 10 μl.

The choice of an injectable anesthetic such as chloral hydrate has several advantages. First, the animal does not need to be ventilated and thus a tracheal tube is not necessary. This makes the surgery quicker and eliminates the risk of asphyxiation from tube blockage. The experimental set-up is simpler as ventilators, and anesthesia analyzers are not necessary. Also, injectable anesthetics pose less risk of accidental exposure to the researcher. Second, the strong odor of inhalatory anesthetics could compromise the integrity of the olfactory pathway, and interfere with application of experimental odors. Thirdly, some mitral cells are entrained with the respiratory cycle [4,20,25,43] and artificial ventilation may interfere with this activity.

However, the application of chloral hydrate was problematic. First, in our surgeries, B6 animals were more prone to accidental overdose. Second, the MOB contains dopamine and the dopamine D2-type receptor [9]. Chloral hydrate both increases dopamine release [24] and alters dopamine–receptor activity [38]. This may partly explain our occasional observations of decreased bulbar spontaneous activity and previous observations of chloral hydrate induced fluctuations in spontaneous activity [16]. It should be noted that several other common anesthetics induced similar changes in bulbar spontaneous activity and dopamine receptor activity [16,38].

Analgesic supplements may reduce the anesthetic load and thus, improve MOB physiology. Our initial attempts with buprenorphine indicated that the MOB, which expresses μ-opioid receptors, is sensitive to μ-opioid agonists. However, non-steroidal anti-inflammatory drugs, such as ketoprofen, may be suitable analgesics for this preparation. Also, as chloral hydrate is applied i.p., the anesthetic plane takes several minutes to change; as such, supplemental doses of anesthetic should be administered several minutes before recording electrical activity (i.e., single-unit activity, EEG). To minimize fluctuations in the anesthetic plane associated with new doses taking effect or older dose wearing off, use fresh chloral hydrate, and monitor the animal consistently so that the smallest possible maintenance doses can be applied.

6.2. Troubleshooting

6.2.1. Excessive bleeding during surgery

To stop excessive bleeding, rapidly apply direct pressure to the wound, for example, with a cotton-tipped applicator. After the bleeding is under control, stop future bleeding with styptic-powder or gel-foam. These agents should be used carefully near neural tissue. When a large volume of blood is lost, physiological saline can be injected i.p. to help prevent dehydration. Prolonged dehydration can alter the pH of cerebral spinal fluid and significantly alter neuronal activity (i.e., seizure). Laceration of the stapedial artery at the TMJ will cause excessive bleeding.

6.2.2. Problems with field potentials

This is usually caused by poor contact of the stimulating electrode to the olfactory nerve fibers or to LOT. Fluid may be shorting out the stimulating electrode. Use twisted strips of laboratory wipes to wick off any fluid. The stimulating electrode may have a poor orientation to the fibers. Make sure the two poles of the electrode are parallel to the fibers, and not perpendicular. Once that is taken care of, try reversing the polarity of the electrical pulse. If the field potential still does not reverse, this may mean that the recording pipette is progressing tangent to the mitral cell layer. This occurs when the pipette is at an edge of the bulb; to fix, move the pipette centrally.

6.2.3. Difficulty in generating antidromic activity

When a candidate mitral cell single-unit has been isolated and is not antidromically driven, make sure the above problems with field potentials are not occurring. After that,

position the antidromic stimulating electrode onto the rostral LOT with a purpose of finding a contact point were the unit is driven. If the unit is driven by LOT stimulation, move the electrode stepwise caudally toward the pPC, and at each step check if the unit is still driven. Continue re-positioning the electrode until it makes contact with the pPC and the unit is driven.

6.3. Alternate protocols

This in vivo protocol can be modified in any of three broad areas: type of anesthetic used, type of recording technique, and type of mitral cell stimulation. First, instead of an injectable anesthetic, inhalatory anesthetics can be applied [7]. Second, instead of extracellular recordings, patch-clamp techniques can be applied [22]. Lastly, instead of electrical stimulation, mitral cells can be stimulated with odors via an olfactometer [42].

The following briefly describes, with representative references, some of the advantages and disadvantages associated with in vitro brain slice preparations. A primary advantage of in vitro brain slices is that neurons can be visually identified. Thus, any class of MOB neuron, or neurons with defined relationships, can be preferentially recorded. For example, juxtaglomerular neurons [2] and adjacent mitral cells [4,41] have been isolated. Also, pharmacological agents can be discretely applied/removed, facilitating detailed analysis of membrane physiology [14,28]. Slice preparations also work well with techniques that use voltage-sensitive dyes [45] or reproduce cellular morphology [14,28].

A primary disadvantage of in vitro brain slice techniques is that the physiology of the tissue may be affected. For example, in vitro mitral cell spontaneous activity differs from in vivo [16]. Even though brain slices are carefully prepared, some neurons undoubtedly die and others are severed. In MOB slice preparations, olfactory receptor neurons are severed and thus, the effects of odorants on MOB neuronal activity cannot be measured. In contrast, the effects of odorants on MOB neuronal activity can be measured in mouse in vivo [3,17,21]. Furthermore, because their axons have been severed, the projections mitral/tufted neurons cannot be determined in vitro. Lastly, in vitro techniques require an extended amount of equipment, for example: a vibrating microtome, an inverted microscope, and reperfusion chambers [14,28].

7. Quick procedure

QP1. Inject mouse with 400 mg/kg of chloral hydrate and apply lidocaine as a local anesthetic.
QP2. Insert ground electrode, i.p. tube, rectal probe and place animal into the stereotaxic.
QP3. Implant the EEG electrode.
QP4. Expose the dorsal MOB surface.

QP5. Expose the posterior piriform cortex and lateral olfactory tract.
QP6. Place the animal into the recording set-up and position the stimulating electrode.
QP7. Insert the recording electrode and keep neural surfaces moist with ACSF and cotton.
QP8. Find desired cell-types based on depth, field potential, and antidromic activation.
QP9. Record spontaneous or evoked activity of MOB neurons.

8. Essential literature references

[4,7,12,21,22,31,36]

References

[1] V. Aroniadou-Anderjaska, M. Ennis, M.T. Shipley, Glomerular synaptic responses to olfactory nerve input in rat olfactory bulb slices, Neuroscience 79 (1997) 425–434.

[2] V. Aroniadou-Anderjaska, F.-M. Zhou, C.A. Priest, M. Ennis, M.T. Shipley, Tonic and synaptically evoked presynaptic inhibition of sensory input to the rat olfactory bulb via $GABA_B$ heteroreceptors, J. Neurophysiol. 84 (2000) 1194–1203.

[3] T. Bozza, J.P. McGann, P. Mombaerts, M. Wachowiak, In vivo imaging of neuronal activity by targeted expression of a genetically encoded probe in the mouse, Neuron 42 (2004) 9–21.

[4] N. Buonviso, M.A. Chaput, F. Berthommier, Temporal pattern analyses in pairs of neighboring mitral cells, J. Neurophysiol. 68 (1992) 417–424.

[5] K.J. Ciombor, M. Ennis, M.T. Shipley, Norepinephrine increases rat mitral cell excitatory responses to weak olfactory nerve input via alpha-1 receptors in vitro, Neuroscience 90 (1999) 595–606.

[6] A. Cowen, Update of the general pharmacology of buprenorphine, in: J. Lewis, A. Cowen (Eds.), Buprenorphine: combating Drug Abuse with an Unique Opioid, Wiley, New York, 1995, pp. 31–47.

[7] J.M. Cuellar, J.F. Antognini, E. Carstens, An in vivo method for recording single unit activity in lumbar spinal cord in mice anesthetized with a volatile anesthetic, Brain Res. Protoc. 13 (2004) 126–134.

[8] J. Ellrich, M. Wesselak, Electrophysiology of sensory and sensorimotor processing in mice under general anesthesia, Brain Res. Protoc. 11 (2003) 178–188.

[9] M. Ennis, F.-M. Zhou, K.J. Ciombor, V. Aroniadou-Anderjaska, A. Hayar, E. Borrelli, L.A. Zimmer, F. Margolis, M.T. Shipley, Dopamine D2 receptor-mediated presynaptic inhibition of olfactory nerve terminals, J. Neurophysiol. 86 (2001) 2986–2997.

[10] K.J. Field, W.J. White, C.M. Lang, Anaesthetic effects of chloral hydrate, pentobarbitone and urethane in adult male rats, Lab. Anim. 27 (1993) 258–269.

[11] T.V. Getchell, G.M. Shepherd, Synaptic actions on mitral and tufted cells elicited by olfactory nerve volleys in the rabbit, J. Physiol. 251 (1975) 497–522.

[12] E.R. Griff, C.A. Greer, F. Margolis, M. Ennis, M.T. Shipley, Ultrastructural characteristics and conduction velocity of olfactory receptor neuron axons in the olfactory marker protein-null mouse, Brain Res. 866 (2000) 227–236.

[13] L.B. Haberly, J.L. Price, The axonal projection patterns of the mitral and tufted cells of the olfactory bulb in the rat, Brain Res. 129 (1977) 152–157.

[14] T. Heinbockel, P. Heyward, F. Conquet, M. Ennis, Regulation of main olfactory bulb mitral cell excitability by metabotropic glutamate receptor mGluR1, J. Neurophysiol. 92 (2004) 3085–3096.

[15] R.B. Jackson, Memorial Laboratory, in: E.L. Green (Ed.), Biology of The Laboratory Mouse by The Staff of The Jackson Laboratory, 2nd ed., McGraw-Hill, New York, 1966, pp. 342.

[16] M. Jiang, E.R. Griff, M. Ennis, L.A. Zimmer, M.T. Shipley, Activation of locus coeruleus enhances the responses of olfactory bulb mitral cells to weak olfactory nerve input, J. Neurosci. 16 (1996) 6319–6329.

[17] D.Y. Lin, S.-Z. Zhang, E. Block, L.C. Katz, Encoding social signals in the mouse olfactory bulb, Nature 434 (2005) 470–477.

[18] C. Linster, M.E. Hasselmo, Behavioral responses to aliphatic aldehydes can be predicted from known electrophysical responses of mitral cells in the olfactory bulb, Physiol. Behav. 66 (1999) 497–502.

[19] K. Lufty, S. Eitan, C.D. Bryant, Y.C. Yang, N. Saliminejad, W. Walwyn, B.L. Keiffer, H. Takeshima, F.I. Carroll, N.T. Maidment, C.J. Evans, Buprenorphine-induced antinociception is mediated by ç-opioid receptors and compromised by concomitant activation of opioid receptor-like receptors, J. Neurosci. 23 (2003) 10331–10337.

[20] F. Macrides, S.L. Chorver, Olfactory bulb units: activity correlated with inhalation cycles and odor quality, Science 175 (1972) 84–87.

[21] T.W. Margie, B. Sakmann, N.N. Urban, Action potential propagation in mitral cell lateral dendrites is decremental and controls recurrent and lateral inhibition in the mammalian olfactory bulb, Proc. Natl. Acad. Sci. 98 (2001) 319–324.

[22] T.W. Margie, M. Brecht, B. Sakmann, In vivo, low-resistance, whole-cell recordings from neurons in the anaesthetized and awake mammalian brain, Pflugers Arch.-Eur. J. Physiol. 444 (2002) 491–498.

[23] P. Mombaerts, F. Wang, C. Dulac, S.K. Chao, M. Mendelsohn, J. Edmondson, R. Axel, Visualizing an olfactory sensory map, Cell 87 (1996) 675–686.

[24] S. Momosaki, K. Hatano, Y. Kawasumi, T. Kato, R. Hosoi, K. Kobayashi, O. Inoue, K. Ito, Rat-PET study without anesthesia: anesthetics modify the dopamine D1 receptor binding in rat brain, Synapse 54 (2004) 207–213.

[25] F. Mototkizawa, Y. Ogawa, Discharge properties of mitral/tufted cells in the olfactory bulb of cats, Brain Res. 763 (1997) 285–287.

[26] W.T. Nickell, M.M. Behbehani, M.T. Shipley, Evidence for GABA$_B$-mediated inhibition of transmission from the olfactory nerve to mitral cells in the rat olfactory bulb, Brain Res. Bull. 35 (1994) 119–123.

[27] B. Pal, A. Por, G. Szucs, I. Kovacs, Z. Rusznak, HCN channels contribute to the intrinsic activity of cochlear pyramidal cells, Cell. Mol. Life Sci. 60 (2003) 2189–2199.

[28] B. Palouzier-Paulignan, P. Duchamp-Viret, A.B. Hardy, A. Duchamp, GABA$_A$ receptor-mediated inhibition of mitral/tufted cell activity in the rat olfactory bulb: a whole-cell patch-clamp study in vitro, Neuroscience 111 (2002) 241–250.

[29] S. Phillips, E.R. Griff, Impulse conduction of olfactory receptor neuron axons, Microsc. Res. Tech. 58 (2002) 161–167.

[30] C.G. Phillips, T.P. Powell, G.M. Shepherd, Responses of mitral cells to stimulation of the lateral olfactory tract in the rabbit, J. Physiol. 168 (1963) 65–88.

[31] P. Popesko, V. Rajtova, J. Horak, A Color Atlas of the Anatomy of Small Laboratory Animals, vol. 2, Wolfe, London, 1992, pp. 109–127.

[32] C. Ron Yu, J. Power, G. Barnea, S. O'Donnell, H.E.V. Brown, J. Osborne, R. Axel, J.A. Gogos, Spontaneous neural activity is required for the establishment and maintenance of the olfactory sensory map, Neuron 42 (2004) 553–566.

[33] J.V. Roughan, P.A. Flecknell, Buprenorphine: a reappraisal of its antinociceptive effects and therapeutic use in alleviating post-operative pain in animals, Lab. Anim. 36 (2002) 322–343.

[34] S.P. Schneider, J.W. Scott, Orthodromic response properties of rat olfactory bulb mitral and tufted cells correlate with their projection patterns, J. Neurophysiol. 50 (1983) 358–378.

[35] S. Schulz, M. Schreff, T. Koch, A. Zimprich, C. Gramsch, R. Elde, V. Hollt, Immunolocalization of two mu-opioid receptor isoforms (mor1 and mor2) in the rat central nervous system, Neuroscience 82 (1988) 613–622.

[36] J.W. Scott, Electrophysiological identification of mitral and tufted cells and distributions of their axons in olfactory system of the rat, J. Neurophysiol. 46 (1981) 918–931.

[37] J.W. Scott, R.L. McBride, S.P. Schneider, The organization of projections from the olfactory bulb to the piriform cortex and olfactory tubercle in the rat, J. Comp. Neurol. 194 (1980) 519–534.

[38] P. Seeman, S. Kapur, Anesthetics inhibit high-affinity states of dopamine D2 and other G-linked receptors, Synapse 50 (2003) 35–40.

[39] J. Silverman, W.H. Muir, Special topic overview: a review of laboratory animal anesthesia with chloral hydrate and chloralose, Lab. Anim. Sci. 43 (1993) 210–216.

[40] Y. Tong, J.-G. Chabot, S.-H. Shen, B.F. O'Dowd, S.R. George, R. Quirion, Ontogenic profile of the expression of the mu opioid receptor gene in the rat telencephalon and diencephalons: an in situ hybridization study, J. Chem. Neuroanat. 18 (2000) 209–222.

[41] N.N. Urban, B. Sakmann, Reciprocal intraglomerular excitation and intra- and interglomerular lateral inhibition between mouse olfactory bulb mitral cells, J. Physiol. 542 (2002) 355–367.

[42] M. Vigouroux, P. Viret, A. Duchamp, A wide concentration range olfactometer for delivery of short reproducible odor pulses, J. Neurosci. Methods 24 (1988) 57–63.

[43] T.A. Young, D.A. Wilson, Frequency-dependent modulation of inhibition in the rat olfactory bulb, Neurosci. Lett. 276 (1999) 65–67.

[44] G.Z. Yu, H. Kaba, H. Saito, K. Seto, Heterogeneous characteristics of mitral cells in the rat olfactory bulb, Brain Res. Bull. 31 (1993) 701–706.

[45] M. Zochowski, M. Wachowiak, C.X. Falk, L.B. Cohen, Y.-W. Lam, S. Antic, D. Zecevic, Concepts in imaging and microscopy: imaging membrane potential with voltage-sensitive dyes, Biol. Bull. 198 (2000) 1–21.